Residual Strength and Damage Mechanisms of Laminated Carbon Fiber Reinforced Polymer under Thermal Environments and Laser Irradiations

Weina Zhao,[1,2] **Yihui Huang**,[3] **Hongwei Song**,[1,2] **Chenguang Huang**[1,2]
[1]*Key Laboratory for Mechanics in Fluid Solid Coupling Systems, Institute of Mechanics, Chinese Academy of Science, Beijing, 100190, China*
[2]*School of Engineering Science, University of Chinese Academy of Sciences, Beijing, 100049, China*
[3]*Ningbo Institute of Industrial Technology, Chinese Academy of Science, Ningbo, 315201, China*

It is interesting to compare the residual strength of laminated carbon fiber reinforced polymer under thermal environments with finite heating rate, and laser irradiation with rapid heating rate. In these two conditions, heating rates are varied in two orders of magnitude, and thermally-induced damage mechanisms are quite different, which may influence the performance of residual strength. Systematic experiments are performed to obtain the tensile failure behavior of laminated carbon fiber reinforced epoxy composites at different temperatures with a heating rate of about 10^{2}°C/min. In comparison, composite samples are subjected to laser irradiations of different power densities and then tested for residual strengths, the laser induced heating rate is above 10^{4}°C/min. Experimental results indicate that the residual strength decreases with the increase of heating temperatures and laser power densities, however the damage mechanisms for conventional heating are thermal pyrolysis, oxidation and delamination, whereas the main damage mechanisms for laser irradiation are thermal pyrolysis and fiber ablation. The experimentally obtained residual strength and modulus are also compared with those predicted by theoretical model. POLYM. ENG. SCI., 58:2311–2319, 2018.

INTRODUCTION

When carbon fiber reinforced polymer (CFRP) composites are heated and subjected to tensile or compressive loadings, their failure behaviors demonstrate some peculiarities and are quite different from those at room temperature. In these cases, CFRP composites undergo thermo-chemical decomposition and irreversible changes of thermo-mechanical properties, which adversely affect the reliability and the load-bearing performance of the structure. The complex chemical and physical process and thermo-mechanical behaviors of the composite exposed to high heat flux or high temperatures have been examined in a number of literatures [1–14], especially in the event of fire [15–22].

Correspondence to: H. Song; e-mail: songhw@imech.ac.cn
Contract grant sponsor: National Natural Science Foundation of China, Contract grant numbers: 91016025, 11332011, 11602271, and 11472276; Contract grant sponsor: National Defense Basic Scientific Research Program of China, Contract grant number: JCKY2016130B009; Contract grant sponsor: Project of the Chinese Academy of Sciences.
DOI 10.1002/pen.24853
Published online in Wiley Online Library (wileyonlinelibrary.com).

Over the years, thermo-mechanical behaviors of composites at thermal environments have been studied and investigated [1–4, 6–14, 23, 24]. Dimitrienko [3, 4] analyzed effects of temperatures and heating rates on thermal properties of matrixes, fibers and composites through thermal experiments and theoretical model, and concluded that the higher the heating rate for heated composites to the same temperature, the smaller the decrease of thermal properties of composites. Bahramian et al. [24] built a model about thermal behaviors of the phenolic resin/asbestos cloth composite to confirm experimental data of oxyacetylene flame tests, which were performed at different heating rates. Shi et al. [12] established a coupled solution model to analyze the thermal and mechanical responses of a silica-phenolic composite exposed to heat flux environments created by oxyacetylene flames, and evaluated the accuracy of the model. Yang et al. [13] used discrete element method to model the interlaminar stress distributions as well as progressive damage propagation in cross-ply laminates under thermal and mechanical loadings, and performed a series of tests of both mechanical and thermal properties of the 0° plies to validate the method. Rupnowski et al. [23] used the Eshelby/Mori–Tanaka method to predict the elastic properties of a unidirectional graphite fiber/polyimide composite for temperatures ranging from 25°C to 315°C, and impacts of heating rates are ignored.

Most previous experimental work aims at the disclosure of the fire behavior of composite specimens or structures, which are typically subjected to one-side heat flux [10, 16, 17, 19, 25–34]. Kandare et al. [10] conducted a series of experiments on the thermo-mechanical responses of fiber-reinforced composites under different temperatures and heating rates (10°C/min or 200°C/min), and used experimental results as input data to validate the kinetic, heat transfer, and thermo-mechanical models. Feih et al. [16] presented a thermo-mechanical model to predict the time-to-failure of polymer laminates loaded in tension or compression and exposed to one-sided radiant heating by using the fire of heat flux levels between 10 and 75 kW/m^2. It was found that the time-to-failure of the laminate decreased with increasing heat flux and increasing applied stress for both the compression and tension load conditions. Firmo et al. [17] performed the experimental and numerical investigations about the fire behavior of reinforced concrete (RC) beams strengthened with CFRP laminates, and developed two-dimensional finite element thermal models to predict the evolution of temperatures in the materials. Dodds et al. [26] investigated the thermal response of laminated glass fiber reinforced panels by fire furnace testing and thermal modeling, and demonstrated the accuracy of the model by measuring the fire resistance of

several matrix materials. Liu et al. [31] analyzed the response of a composite column under combined single-sided surface heating and compression loadings, and examined the time-to-failure and failure mode of a vinyl-ester/glass composite exposed to fluxes of 25 kW/m^2, 50 kW/m^2, and 75 kW/m^2. Shi et al. [32] presented a mesomechanical model to explain the degraded behavior of FRP composites exposed to one-sided heat flux (100 kW/m^2 and 200 kW/m^2) under static compressive loadings, and concluded that the degradation in stiffness properties of the composite occurs due to the thermal decomposition of polymer matrix and phase transition of reinforced fibers at higher temperatures. Wang et al. [34] proposed a segmented model to describe the tensile strength of CFRP pultruded strips at high temperatures, and revealed the significant difference of various heating rates (5°C/min∼25°C/min) on the material properties.

It is found that the mechanical performance of polymer composite depends not only on temperature but also on the time exposed to high temperatures, or heating rates. Most previous experiments use an input heat flux in the level of 10^2 kW/m^2, and the heating rate in the level of 10^2°C/min. When the composite is irradiated by a high power laser, however, the input heat flux can reach 10^2 MW/m^2, and the heating rate is beyond 10^4°C/min. It is interesting to compare the damage mechanisms and residual strength of composite at finite heating rate and very rapid heating rate. This article presents an experimental study on the failure behavior of CFRP composites subjected to tensile under thermal environments and laser irradiations. Mechanisms of thermally-induced damages are discussed, and residual strength variations with thermal load are compared for these two conditions. The experimentally obtained residual strength and Young's modulus under conventional thermal environments are also compared with those predicted by recently developed theoretical model.

EXPERIMENTAL PROCEDURE

Specimen Preparation

In the present study, the laminated CFRP composites with epoxy matrix, i.e., T700/BA9916 are tested. The CFRP composites are fabricated and provided by AVIC Composite Corporation Ltd. The curing temperature for T700/BA9916 epoxy prepreg is 180°C. Characterized by the high curing tempreature (180°C) and high toughness, BA9916 epoxyis is used as the resin hardener for T700/BA9916 epoxy prepreg. During preparation, prepreg tapes are heated to 180°C at the rate of 0.3°C/min-3°C/min, and kept in this specific temperature for 180 min, then dropped to the room temperature at the maximum rate of 2°C/min. Mechanical properties of unidirectional prepreg tapes are shown in Table 1. The ply pattern of laminated composites is designed as $[45°/0°/–45°/90°]_{2S}$. Taking advantage of the excellent processing technology, the porosity volume fraction is usually no more than 0.01 and therefore can be neglected. In terms of the volume ratio, the epoxy and fibers in the laminated composites accounts for 0.467 and 0.533, respectively. The lamina thickness is 0.150 mm, the total thickness of the laminated CFRP is 2.40 mm, and the width is 20 mm. Samples are prepared according to ASTM standards (D 3039/D 3039M for tensile tests).

TABLE 1. Properties of unidirectional prepreg tapes.

Properties	T700/BA9916	
Mechanical properties (Room temperature)	0°Tensile strength, MPa	1,489
	0°Tensile modulus, GPa	132.8
	90°Tensile strength, MPa	58.5
	90°Tensile modulus, GPa	9.7
	Shear strength, MPa	121
	Shear modulus, GPa	5.3
Thermal properties	Density, g/cm^3	1.54
	Specific heat, J/(kg·°C)	1,038

Tensile Tests at Thermal Environments

In tensile tests at thermal environments, electric resistance wire is utilized to provide heat source. The electric resistance wire is flexible to be wound into a heating band, which is set around the specimen and fixed in the testing machine. The main advantage of this method is its simplicity in providing a local heating to the testing region, meanwhile it keeps the strengthening and clamping regions unaffected. The heating rate can be readily altered by adjusting the voltage. Thermal couples of NiCr-NiSi type are installed to monitor the temperature of specimen as well as the heating rate. A DIC system is utilized to obtain the tensile strain. Speckles are sprayed at the end of the specimen, easy to be captured by the CCD. During the test, the sampling frequency of the CCD is 5 frames per second. Loading rates are set at 2 mm/min for tension tests. At the beginning of test, the specimen is fixed in the test machining and heated to a target temperature. While maintaining the target temperature, tensile loading is applied to the specimen through the displacement of crosshead, till the specimen is failed.

Tensile Tests after Laser Irradiation

In comparison with tensile tests at conventional thermal environments, tensile tests after laser irradiation are performed. First, CFRP specimens are irradiated by CW laser of different power densities in a nitrogen protection environment. This is because severe combustion may occur when the CFRP composite is subjected to high heat flux in oxidation environment. A YLS 1,070 nm fiber laser of 2 kW provided by IPG Ltd. is utilized as the laser source. The laser beam irradiates on the center of testing zone with a fixed diameter of 10 mm, and the power density can be varied by changing the output of laser power. In the experiments, samples are irradiated by a power density of 1.5 MW/m^2, 2.5 MW/m^2, 6.3 MW/m^2, 10.1 MW/m^2, and 12.7 MW/m^2 for 3 s, respectively. Then, the defective specimen is applied tensile loading at rate of 2 mm/min in MTS, till the specimen is failed.

Thermal Gravimetric Analysis Tests under Different Environments

Mass loss behavior of composite material due to thermal decomposition are governed by the Arrhenius kinetic formula, in which thermal decomposition kinetic parameters can be obtained from thermal gravimetric (TG) tests. TG tests are performed by using Perkin Elmer Pyris Diamond TG/DTA, at a heating rate of 5°C/min, 25°C/min, and 60°C/min in a nitrogen environment, and 5°C/min and 25°C/min in an oxidation environment, respectively. Based on TG results, thermal damage

mechanisms of CFRP composites under different environments can be derived.

RESULTS AND DISCUSSIONS

Heating Rates and Residual Strengths

To compare the tensile results of laminated CFRP under thermal environments with that under laser irradiations, different heating rates are considered and investigated. Figure 1a gives the temperature rising histories and heating rates at various target temperatures in conventional thermal environments. The heating rate is typically around 10^2°C/min for a high target temperature (above 300°C), whereas at a relative low target temperature, the heating rate is a little lower, e.g., 63°C/min for the target temperature of 124°C. Figure 1b is the measured temperature of back surface opposite to the laser spot center at 3 s irradiation moment. The average heating rate of back surface can be calculated for different laser power densities. Although the back surface temperature is typically around 200°C, the average heating rate can reach 3,000°C/min. SEM image given in the next section indicates that in the laser irradiated zone carbon fibers are ablated into needle clusters, indicating a temperature rise to the sublimation temperature of about 3,000°C. Therefore, the calculated average heating rate of CFRP under laser irradiation is at least in the order of 10^4°C/min, which is two orders of magnitude larger than conventional heating.

Figure 1b also indicates the back surface temperature first rises rapidly with the increase of laser power density and then the tendency is slowed down when laser power density is larger than 2.5MW/m^2. This phenomenon dues to the delamination initiated at nonpyrolysis region at high power densities, which is

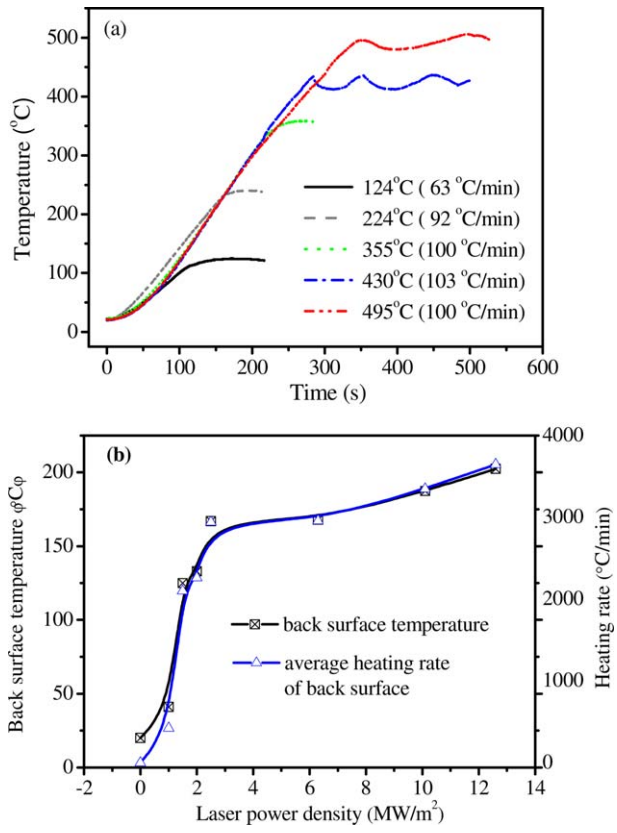

FIG. 1. Comparison of heat rates. (a) uniform thermal environment; (b) local laser irradiation. [Color figure can be viewed at wileyonlinelibrary.com]

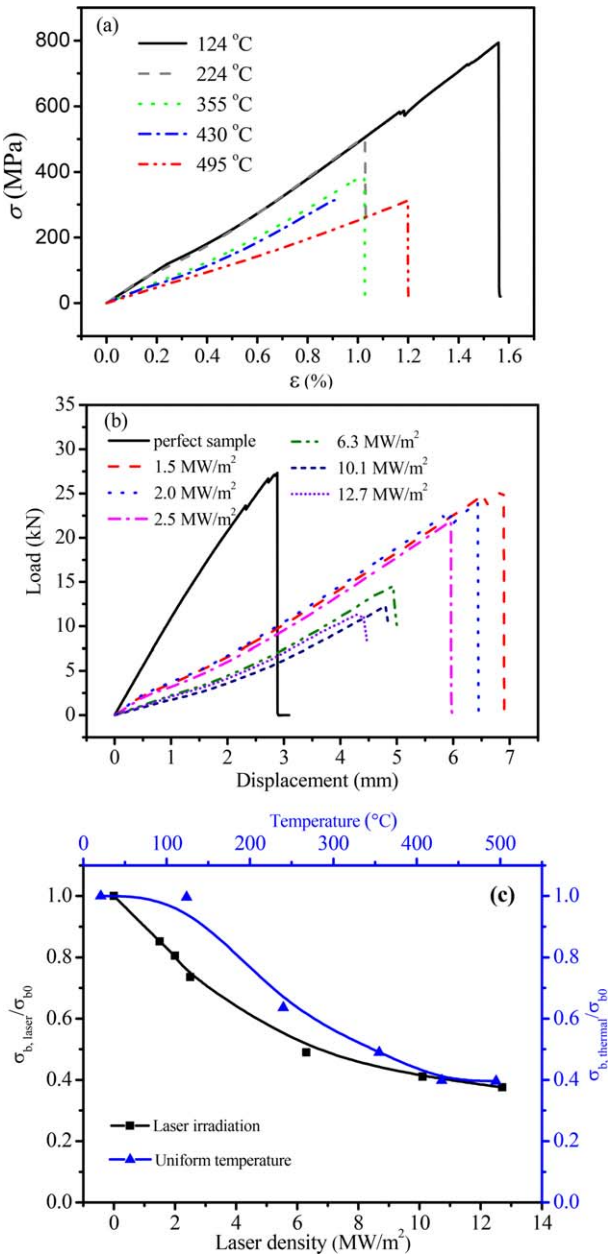

FIG. 2. Comparison of tensile behavior and residual strength. (a) Stress-strain curves at uniform thermal environment; (b) Load-displacement curves after laser irradiation; (c) Residual strengths. [Color figure can be viewed at wileyonlinelibrary.com]

detailed in the section "Laser induced damages". Thermal resistance due to delamination delayed the laser energy to be conducted to the back face.

Once CFRP composites are exposed to thermal loadings, complex thermal damages may occur, which have great influence on mechanical properties of the composites. One of the important properties is the residual strength of the composites. Figure 2 shows the tensile behavior and residual stress of CFRP laminate under thermal environments and laser irradiations. Figure 2a gives stress-strain curves at elevated and high temperatures. Due to the increasing effect of thermal decomposition, both Young's modulus and failure strength decrease with the elevation of target temperatures. Figure 2b compares the tensile load-displacement curves of perfect sample and samples irradiated by different laser

power densities. It is obvious that the mechanical properties of CFRP laminates are significantly affected by the defects caused by laser irradiation. Figure 2c shows dimensionless residual strengths versus different temperatures and laser power densities. $\sigma_{b,laser}$, $\sigma_{b,thermal}$ represents the tensile strength under laser irradiations and thermal environments respectively; σ_{b0} represents the tensile strength of perfect specimen at room temperature. In both cases, residual strength declines as target temperature or laser power density increases. There is a plateau zone of temperature curve before 200°C, which is the thermal pyrolysis activation temperature for epoxy resin. This means the strength maintains relative high before thermal pyrolysis start [35]. The strength decreases sharply as the laser power density increases before it reaches 6.3MW/m^2, after that residual strength decreases slowly.

These two tests can also be compared in the domain of absorbed energy. For tests performed in conventional thermal environments, the absorbed energy can be obtained based on heating history and thermal properties of composites. For the cases of laser irradiation, the absorbed energy can be obtained simply by input laser energy corrected by absorption coefficient. The absorbed energy for laser irradiation is typical 10^{-1} kJ (within 1.0 kJ), whereas it is several kJ (up to 5 kJ) for conventional heating. Although the absorbed energy is lower, the strength degradation tendency due to laser irradiation is more obvious.

Damage Mechanisms

Thermal Decomposition Analysis Based on TG Tests. When CFRP composite with epoxy matrix is exposed to thermal environment, complex chemical and physical processes including pyrolysis of matrix, formation and growth of pores and char, oxidation of residual char and carbon fibers, thermal expansion and contraction, matrix cracking, and delamination may occur [36]. The extent of thermal decomposition depends on exposing temperature, lasting time as well as the environments. To describe the mass-loss behavior of CFRP composites under high temperatures, an Arrhenius-Equation based model with multi-step decomposition was adopted [37]

$$\frac{\partial(m/m_0)}{\partial t} = -J_0\left(\frac{m-m_r}{m_0}\right)^n \exp\left(-\frac{E_A}{R\theta}\right) \tag{1}$$

where J_0, E_A, and n are the pre-exponential factor, activation energy of the thermal decomposition process, and order of the reaction, respectively. m_0 is the initial mass of the material, m is the mass of the material at the thermal decomposition time, m_r is the remaining mass after thermal decomposition, and R is the gas constant, and θ is temperature.

By integration of *Eq. 1*, the effects of temperature and heating rates on the composites mass-loss are derived

$$m/m_0 = \begin{cases} \dfrac{m_r}{m_0} + \dfrac{m_0-m_r}{m_0}\exp\left[\dfrac{-J_0RT^2}{E_A\dot{\theta}}\exp\left(\dfrac{-E_A}{R\theta}\right)\right], & n=1 \\ \dfrac{m_r}{m_0} + \left[\left(\dfrac{m_0-m_r}{m_0}\right)^{1-n} + \dfrac{(n-1)J_0RT^2}{E_A\dot{\theta}}\exp\left(\dfrac{-E_A}{R\theta}\right)\right]^{\frac{1}{1-n}}, & n\neq 1 \end{cases} \tag{2}$$

where, $\dot{\theta}$ represents the heating rate. According to *Eq. 2*, thermal decomposition of CFRP composites is severely affected by the heating rates.

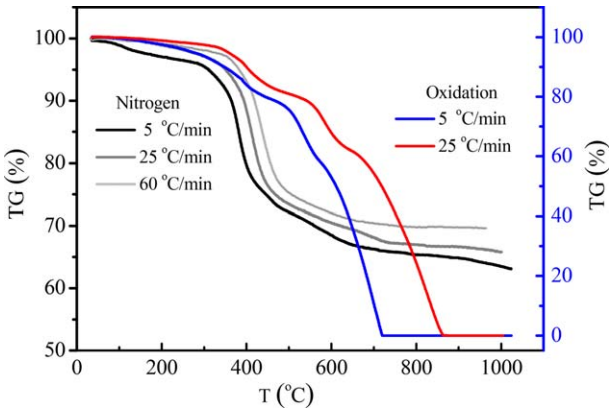

FIG. 3. TG tests under nitrogen and oxidation environments at different heating rate. [Color figure can be viewed at wileyonlinelibrary.com]

Generally, heating rate with 10^{0}°C/min ~10^{2}°C/min is recommended for TG tests. Figure 3 shows the TG result of CFRP composites under nitrogen and oxidation environments at different heating rates. It can be found the lower the heating rate, the more complete the composite is decomposed at the same temperature. In the Nitrogen environment, the remaining mass is larger than 50 percent, which indicates thermal decomposition of carbon fibers can hardly occur. Thermal decomposition behavior is mainly determined by the pyrolysis of epoxy matrix, whose pyrolysis temperature is about 300°C. By contrast, in the oxidation environment, the decomposition behavior of the composite is more complex. Due to the oxidizing process of char and carbon fibers, both matrix and fibers are fully decomposed at the end of TG test.

TG data at the heating rate comparable to laser irradiation is not available. However, processes of thermal decomposition in a nitrogen environment are similar to the aforementioned TG tests. When the temperature is below 1,000°C, CFRP composites mainly undergo process of matrix pyrolysis, and residual char and carbon fibers remain. When the temperature is over 3,000°C, sublimation of carbon fibers occurs.

Thermally Induced Damages in High Temperature Environments. Under the conventional thermal environments, processes of thermal damages can completely act because of the relatively low heating rates. Figure 4 gives the thermally induced morphology of the polymer composite at different target temperatures. When the specimen is heated to 300°C, matrix pyrolysis begins and significant fume and smoke is generated. At the temperature of 400°C, matrix pyrolysis is accelerated, delamination as well as intra-laminar cracks becomes obvious. When the specimen is heated to 500°C, the specimen is completely delaminated and the discrete laminas with intra-laminar cracks demonstrate thermally induced curling. If we continue to increase the temperature, accelerated matrix decomposition, fiber oxidization, and prominent chars and pores can be observed.

Laser Induced Damages. Compared with the thermal damages of CFRP composites under conventional thermal environments, pyrolysis of matrix, and sublimation carbon fibers occur. To describe the thermal damage behavior of CFRP composites irradiated by different laser power densities, morphologies are

 DOI 10.1002/pen

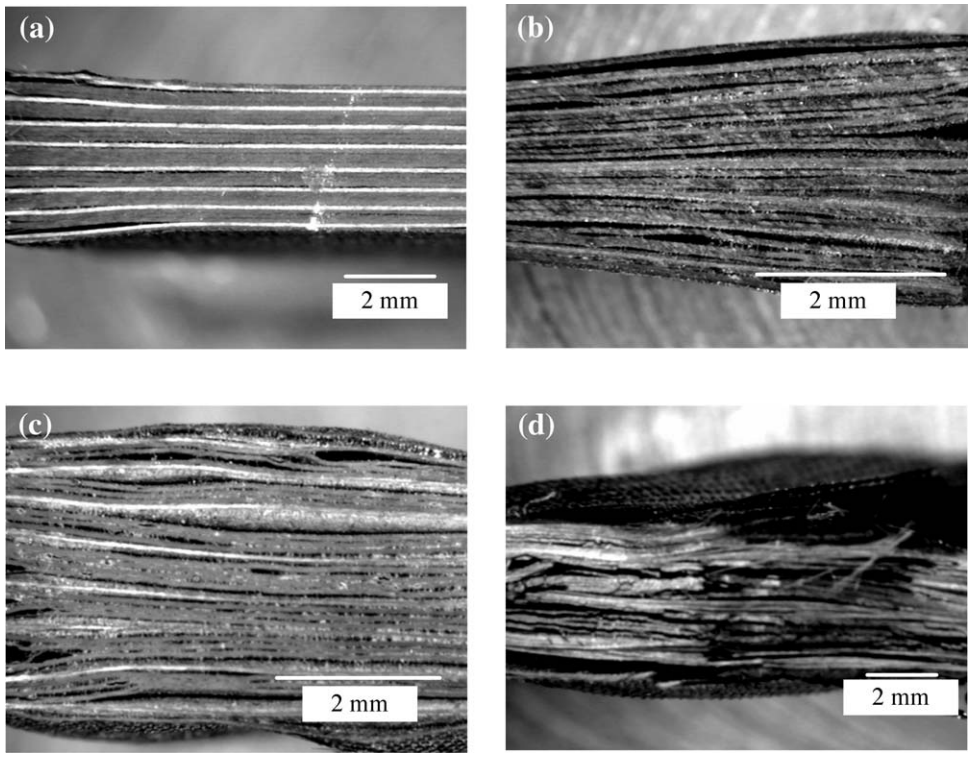

FIG. 4. Thermal behaviors of laminated CFRP composite at different temperatures, at the heating rate of about 100°C/min. (a) $T = 300$°C, fume and smoke generated; (b) $T = 400$°C, matrix pyrolysis, delamination and intra-laminar cracks; (c) $T = 500$°C, delamination with thermal induced curling; (d) $T > 500$°C, fiber oxidization, char and pores.

picked by the Stemi Sv11 stereoscopic microscope. Figure 5 gives the damage profiles of CFRP composites subjected to laser irradiation for 3 s at different power densities. Top view images show that thermal affected regions are approximately elliptical, because the coefficient of thermal conductivity in fiber direction is larger than that of transverse direction. The extent of damage increases with laser power density. When the laser power density reaches 1.5 MW/m^2, the pyrolysis process becomes obvious. The side view of Fig. 5b presents interlaminar crack in the nonpyrolysis region initiated at the laser power density of 2.5 MW/m^2. The delamination behaivor becomes promenient as laser power denisty increases, see the side views of Fig. 5c–e. This damage mechanism can explain the tendency of back surface temperature versus power density given in Fig. 1b: thermal resistance due to interlaminar cracks significantly declays thermal conduction of deposited laser energy to the back surface of laminated CFRP. Therefore, the temperature of back surface rises slowly when laser power density is larger than 2.5 MW/m^2. When the laser power density reaches 10.1 MW/m^2, the carbon fiber is sublimated and cracked.

To characterize thermal damages induced by laser irradiations, the thermal affected area and the thickness of the thermal affected region in relation to laser power density are considered, as shown in Fig. 6. A and N depict the thermal affected area on the laser irradiation surface and the thickness of the thermal affected region, respectively. A_0 represents the thermal affected area of CFRP composites at the laser power density of 1.5 MW/m^2. N_0 is the total thickness of laminated composite. The thermal affected area and thickness increase with laser power density sharply before 2.5MW/m^2, then become stable. The turning point of 2.5MW/m^2 is the laser power density at which delamination cracks occur.

Figure 7 shows the SEM view of CFRP composites irradiated by high power laser (12.7 MW/m^2). Distinct thermal pyrolysis region and unaffected region can be observed in Fig. 7a. In the thermal pyrolysis region, epoxy matrix is almost decomposed, leaving bare fibers almost unbundled. Figure 7b shows that in the laser irradiated zone thermal decomposition of epoxy matrix is almost completed, carbon fibers are ablated into needle clusters, which means rapid sublimation of the carbon fiber due to extremly high heat flux.

Tensile Failure Mechanism at Thermal Environment and Laser Irradiation. From section "Heating Rates and Residual Strengths", obvious difference of residual strengths between thermal environments and laser irradiations can be found. Thus it is necessary to investigate tensile failure mechanisms of CFRP laminates at thermal environment and laser irradiation. Figure 8 illustrates tensile failure modes of CFRP laminates at high temperatures. As shown in Fig. 8, the failure mode of CFRP laminates at a moderate temperature (e.g., 124°C) is similar to that of room temperature, which is a complete fracture in carbon fibers and epoxy matrix through thickness. Figure 8b is the image of enlarged fracture band failed at 124°C. The epoxy matrix is softened and melted when the temperature rises. As a result, the bonding strength is weakened. The intra-laminar and inter-laminar cracks are formed and propagated during the acceleration of matrix pyrolysis and residual char oxidation

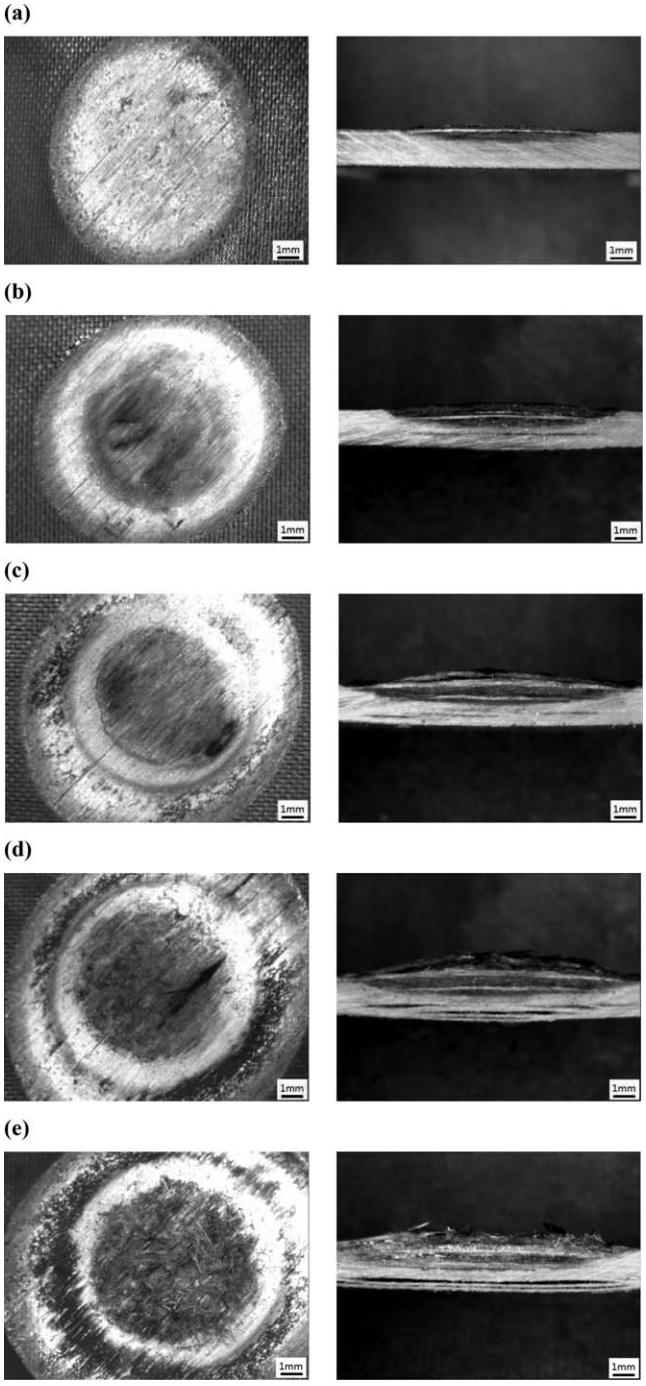

FIG. 5. Damage morphology of CFRP after laser irradiation for 3 s. On the left is top view, and on the right is side view. (a) 1.5 MW/m^2; (b) 2.5 MW/m^2; (c) 6.3 MW/m^2; (d) 10.1 MW/m^2; (e) 12.7 MW/m^2.

under high temperatures, which result in significant degradation in mechanical properties. In Fig. 8c, melted matrix, broken bare fibers and residue char can be found for the specimen failed at the temperature of 430°C.

For the detailed analysis of tensile damage mechanism of CFRP composites at high temperature, the SEM view is displayed in Fig. 9. It can be concluded that main tensile failure mechanisms are delamination, fiber/matrix debonding, and fiber breakage.

In contrast with failure modes of CFRP laminates under conventional thermal environments, tensile failure modes of

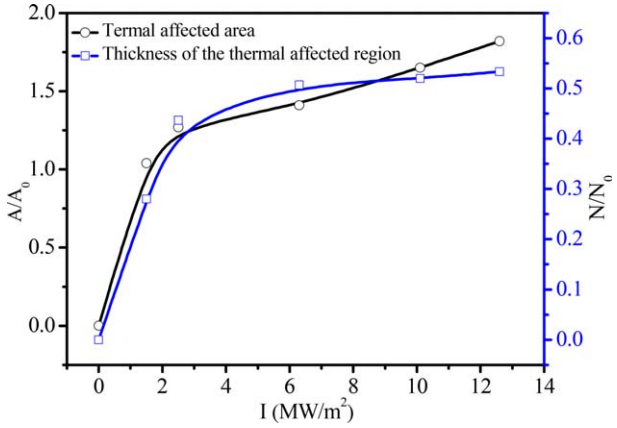

FIG. 6. The variations of thermal affected area and thickness with respect to laser power density. [Color figure can be viewed at wileyonlinelibrary.com]

CFRP laminates under laser irradiations were also investigated. Figure 10 shows tensile failure modes of CFRP laminates under laser irradiation of different power densities. Samples are failed in the middle of testing zone, where laser

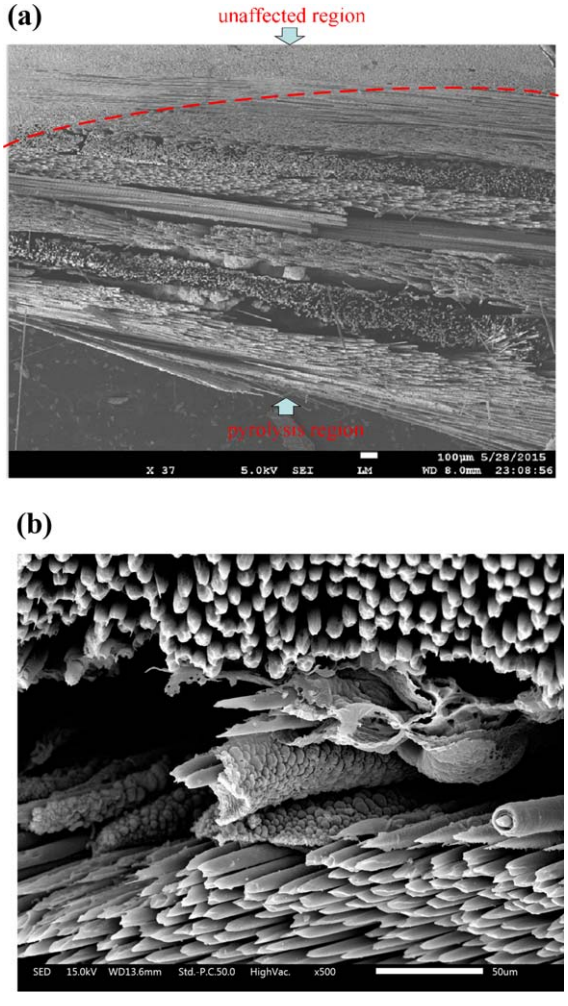

FIG. 7. SEM pictures of intense laser induced damages. (a) local thermal pyrolysis region; (b) needle clusters of carbon fiber after laser ablation. [Color figure can be viewed at wileyonlinelibrary.com]

DOI 10.1002/pen

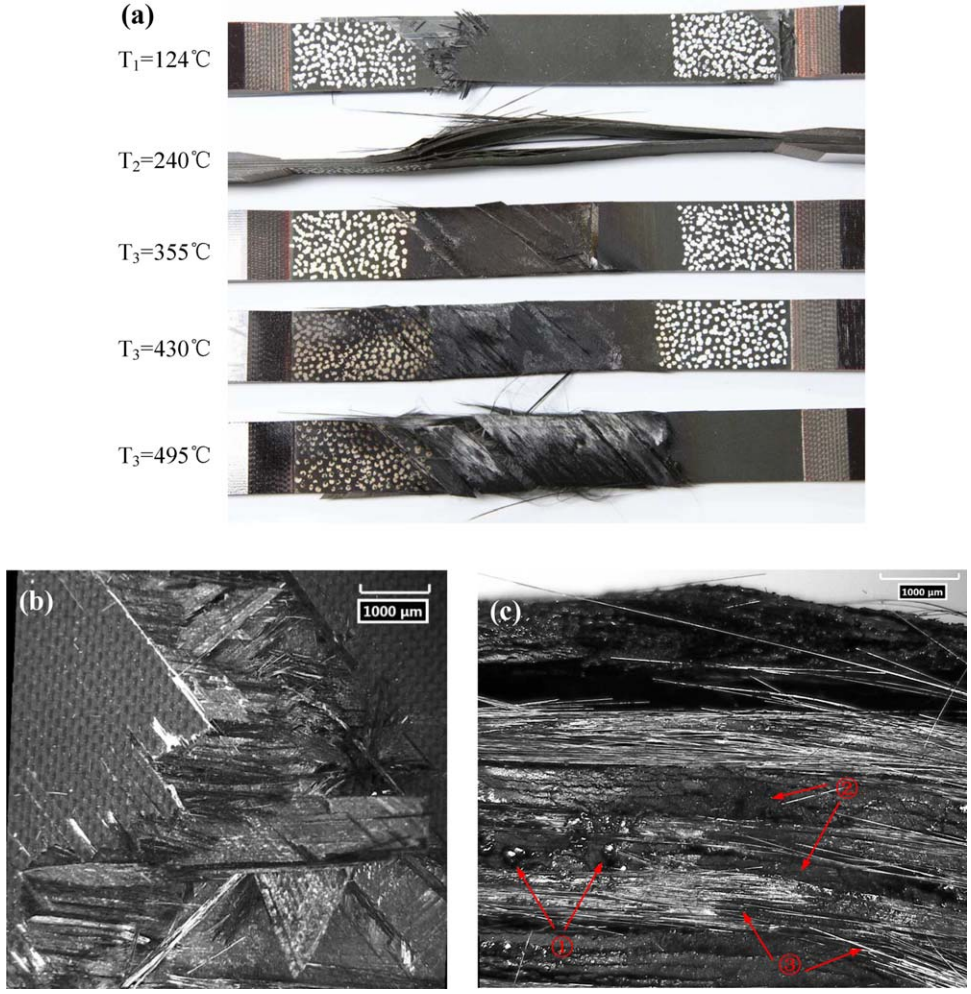

FIG. 8. Tensile failure modes of CFRP laminates at elevated and high temperatures. (a) failure region of the tested specimen; (b) $T = 124$℃, fiber and matrix fracturing; (c) $T = 430$℃, ①melted matrix, ②residue char, ③broken fibers. [Color figure can be viewed at wileyonlinelibrary.com]

spot located. Defects produced by laser irradiation induced stress concentration, where fracture initiates during tension. Mass loss due to ablation and sublimation of both matrix and fiber under high heat flux, together with insufficient thermal pyrolysis and delamination accounts for reduction of tensile strength.

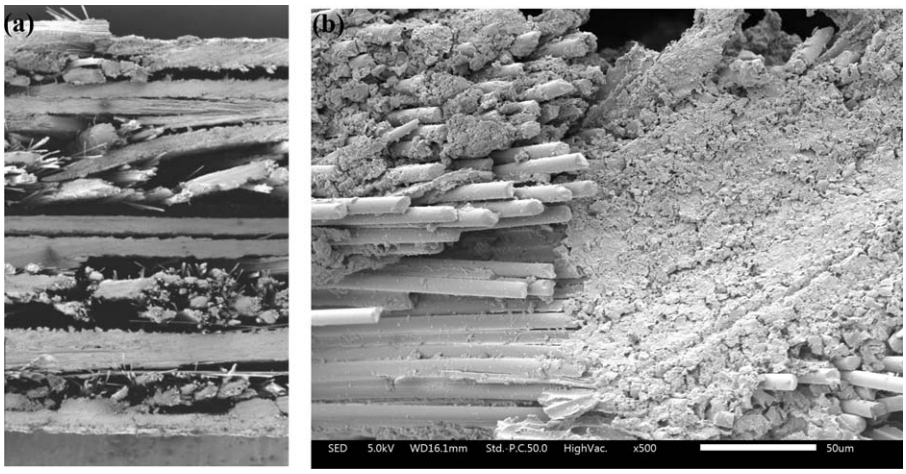

FIG. 9. SEM view of tensile failure mechanisms of CFRP composites under thermal environment. (a) delamination; (b) debonding and fiber breakage.

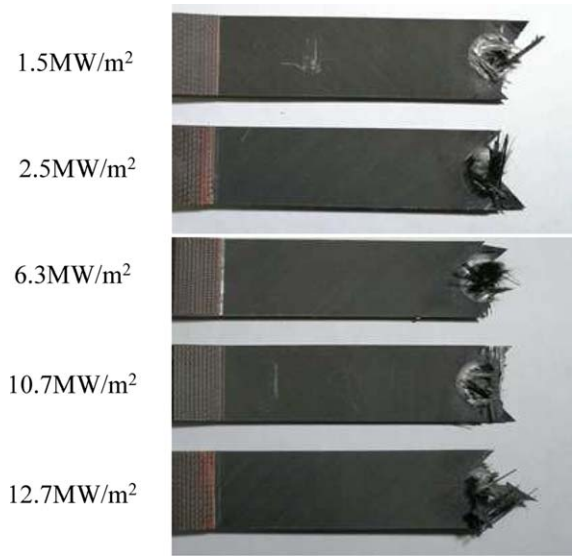

FIG. 10. Tensile failure modes of CFRP laminates under laser irradiations. [Color figure can be viewed at wileyonlinelibrary.com]

Comparison with Theoretical Predictions

Experimental results in thermal environments are also compared with predictions from a recently developed theoretical model [36]. First, a mesoscopic to macroscopic model, considering thermal degradation of both matrix and fibers, is established to obtain the thermo-mechanical properties of the CFRP composite subject heating. Thermal degradation of CFRP follows the Arrhenius kinetic formula, and thermo-physical properties and mechanical properties are determined as functions of the temperature and the heating rate. Second, a progressive destruction program based on the classical laminate theory is built, and thermo-mechanical properties of the decomposed composite are input as defects to the initial stiffness matrix. Then residual strengths of CFRP at various heating rate and temperature can be solved. Mechanical properties of unidirectional prepreg tapes at room temperature used in the analytical model are listed in Table 1.

For laminated composites, the prediction of failure depends on stress in each single lamina. Theoretically, the failure

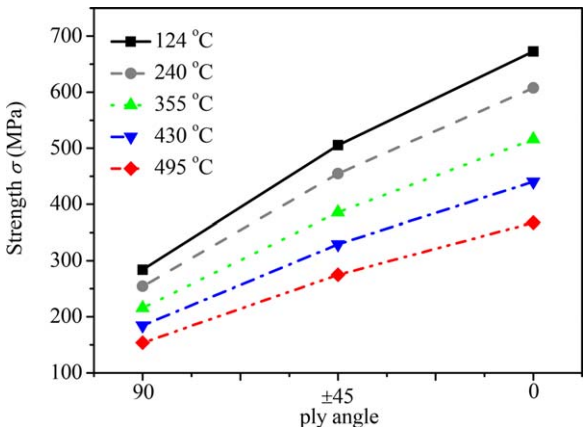

FIG. 11. Theoretically predicted failure modes and failure strength, heating rate of about 100°C/min. [Color figure can be viewed at wileyonlinelibrary.com]

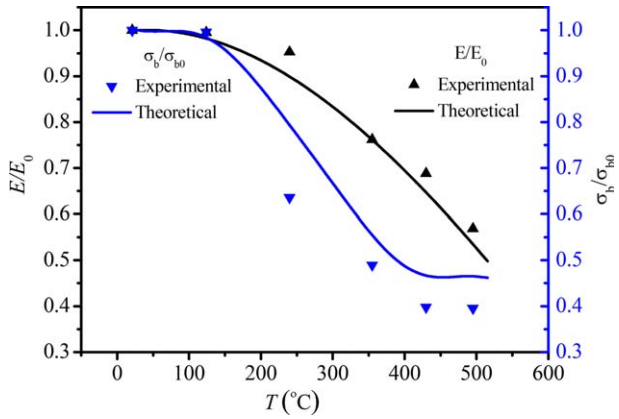

FIG. 12. Comparison of theoretical and experimental results about dimensionless Young's modulus and residual strength. [Color figure can be viewed at wileyonlinelibrary.com]

prediction of single lamina in laminated composites can be readily achieved using Tsai-Hill criterion which is expressed as follows

$$\frac{\sigma_1^2}{X^2}-\frac{\sigma_1\sigma_2}{X^2}+\frac{\sigma_2^2}{Y^2}+\frac{\tau_{12}^2}{S^2}=1 \tag{3}$$

where X, Y, and S are longitudinal strength, transverse strength and shear strength, respectively. This criterion is well suited for the composite where tensile strength and compressive strength are the same. After calculating the predicted failure of each single lamina, the whole failure prediction of CFRP laminated composites at high temperatures can be derived.

As [45°/0°/–45°/90°]2S laminate has quasi-isotropic property, the theoretically predicted equivalent Young's modulus and Poisson's ratio of the laminated composite can be derived from *Eq. 4*.

$$\begin{aligned} E&=\frac{(E_1+E_2)^2-4v_{21}^2E_2^2+4G_{12}(1-v_{12}v_{21})(E_1+E_2+2v_{12}v_{21})}{[3E_1+3E_2+2v_{21}E_2+4G_{12}(1-v_{12}v_{21})](1-v_{12}v_{21})}\\ v&=\frac{E_1+E_2+6v_{21}E_2-4G_{12}(1-v_{12}v_{21})}{3E_1+3E_2+2v_{21}E_2+4G_{12}(1-v_{12}v_{21})} \end{aligned} \tag{4}$$

Theoretically predicted failure modes are shown in Fig. 11. Specimens at elevated and high temperatures fail in a progressive damage way, with the failure sequence of 90° plies, ±45° plies and 0° plies. In some experimental results, e.g., stress-strain curve of 124°C in Fig. 1a, obvious drop in stress can be found at the strain of about 1.2%, indicating a progressive fracture of the laminate.

Figure 12 presents the comparison of experimental and theoretical results at the heating rate of about 100°C/min in an oxidation environment. The analytical model includes thermal decomposition behaviors of epoxy matrix, thermal oxidization behaviors of carbon fibers, as well as progressive destruction of the laminated composite. The predicted Young's modulus and residual strength decays with target temperature, which is in accordance with experimental observation.

CONCLUSIONS

Thermal-mechanical response of CFRP composites depends not only on temperature but also on heating rates, or duration of

DOI 10.1002/pen

heating. In the experiment of conventional thermal environment, the tested zone of CFRP samples are uniformly heated to a temperature up to 500°C at a heating rate of about 10^{2}°C/min. In contrast, under high power laser irradiation the local temperature may reach 3,000°C in 3 s, and the heating rate is beyond 10^{4}°C/min. Although experimental results indicate that the residual strength decreases with the increase of target temperatures and laser power densities, mechanisms of thermally-induced damage are quite different. In the conventional heating environments, the samples are sufficiently decomposed, and thermal pyrolysis of epoxy matrix, oxidation of residual char, intra-layer crack and inter-layer delamination are the main damage mechanisms. Whereas for samples subjected to laser irradiation, mass loss due to ablation and sublimation of both epoxy matrix and carbon fibers produces local defect. The local ablation behavior together with insufficient thermal pyrolysis of epoxy matrix, intra-layer crack and inter-layer delamination accounts for the reduction of tensile strength.

REFERENCES

1. S.K. Bapanapalli, B.V. Sankar, and R.J. Primas, *J. AIAA*, **44**, 2949 (2006).
2. X. Chang, Z. Li, T. Chen, and P. Fang, *Infrared Laser Eng*., **40**, 1936 (2011).
3. Y. Dimitrienko, *Appl. Compos. Mater*., **4**, 219 (1997).
4. Y. Dimitrienko, *Compos. Part A-Appl. Sci*., **28**, 453 (1997).
5. J-L. Gao and J-S. Yu, *Fiber Compos*., **3**, 014 (2005).
6. N. Guermazi, N. Haddar, K. Elleuch, and H.F. Ayedi, *Mater. Design*, **56**, 714 (2014).
7. G.E. Hassani Nezhad, M. Malaska, and K. Kujala, *Eng. Struct*., **75**, 363 (2014).
8. C. Henaff-Gardin, I. Goupillaud, and M.C. Lafarie-Frenot, *Evolution of matrix cracking in cross-ply CFRP laminates: Differences between mechanical and thermal loadings*, 4th International Conference on Durability Analysis of Composite Systems, Brussels, Belgium (2000).
9. P. Ifju, D. Myers, and W. Schulz, *Compos. Sci. Technol*., **66**, 2449 (2006).
10. E. Kandare, B.K. Kandola, E.D. McCarthy, P. Myler, G. Edwards, J.F. Yong, and Y.C. Wang, *J. Compos. Mater*., **45**, 1511 (2011).
11. E. Nassiopoulos and J. Njuguna, *Mater. Design*, **66**, 473 (2015).
12. S. Shi, J. Liang, G. Lin, and G. Fang, *Compos. Sci. Technol*., **87**, 204 (2013).
13. Yang D, Sheng Y, Ye J, and Tan Y, *Multi-scale modeling of the progressive damage in cross-ply laminates under thermal and mechanical loading*, International Conference on Structural Nano Composites, Cranfield University, England (2012).
14. A.M. Zenkour, M.N.M. Allam, and A.F. Radwan, *Int. J. Mech. Mater. Des*., **9**, 239 (2013).
15. U. Berardi and N. Dembsey, *Polymers*, **7**, 2276 (2015).
16. S. Feih, Z. Mathys, A.G. Gibson, and A.P. Mouritz, *Compos. Sci. Technol*., **67**, 551 (2007).
17. J.P. Firmo, J.R. Correia, and P. Franca, *Compos. Pt B-Eng*., **43**, 1545 (2012).
18. A.G. Gibson, Y.S. Wu, J.T. Evans, and A.P. Mouritz, *J. Compos. Mater*., **40**, 639 (2006).
19. E. Kandare, G.J. Griffin, S. Feih, A.G. Gibson, B.Y. Lattimer, and A.P. Mouritz, *Compos. Part A-Appl. Sci*., **43**, 793 (2012).
20. L. Liu, J.W. Holmes, G.A. Kardomateas, and V. Birman, *Fire Technol*., **47**, 985 (2009).
21. M.T. McGurn, P.E. DesJardin, and A.B. Dodd, *Int. J. Heat Mass Tran*., **55**, 272 (2012).
22. A.P. Mouritz, S. Feih, E. Kandare, Z. Mathys, A.G. Gibson, P.E. Des Jardin, S.W. Case, and B.Y. Lattimer, *Compos. Part A-Appl. Sci*., **40**, 1800 (2009).
23. P. Rupnowski, M. Gentz, and M. Kumosa, *Compos. Sci. Technol*., **66**, 1045 (2006).
24. A.R. Bahramian, M. Kokabi, M.H.N. Famili, and M.H. Beheshty, *Polymer*, **47**, 3661 (2006).
25. Y. Dimitrienko, *Compos. Part A-Appl. Sci*., **31**, 591 (2000).
26. N. Dodds, A.G. Gibson, D. Dewhurst, and J.M. Davies, *Compos. Part A-Appl. Sci*., **31**, 689 (2000).
27. S. Feih, Z. Mathys, A.G. Gibson, and A.P. Mouritz, *Compos. Part A-Appl. Sci*., **38**, 2364 (2007).
28. J.P. Firmo and J.R. Correia, *Compos. Pt B-Eng*., **76**, 112 (2015).
29. P.K. Gotsis, C.C. Chamis, and L. Minnetyan, *Compos. Sci. Technol*., **58**, 1137 (1998).
30. B.K. Kandola, P. Luangtriratana, S. Duquesne, and S. Bourbigot, *Materials*, **8**, 5216 (2015).
31. L. Liu, J.W. Holmes, G.A. Kardomateas, and V. Birman, *Fire Technol*., **47**, 985 (2011).
32. S.B. Shi, L.X. Gu, J. Liang, G.D. Fang, C.L. Gong, and C.X. Dai, *Mater. Design*, **89**, 1079 (2016).
33. C.T. Sun, J. Tao, and A.S. Kaddour, *Compos. Sci. Technol*., **62**, 1673 (2002).
34. K. Wang, B. Young, and S.T. Smith, *Eng. Struct*., **33**, 2154 (2011).
35. N. Zhang, C. Liu, and C. Sun, *The thermocoupling effect of CW COIL beam on composites*, 26th AIAA Plasmadynamics & Lasers Conference, San Diego (1995).
36. W.N. Zhao, H.W. Song, C.G. Huang, and Y.H. Huang, *Int. J. Appl. Mech*., **9**, 25 (2017).
37. M. Chen, H. Jiang, and Z. Liu, *High Power Laser Part. Beams*, **22**, 1969 (2010).